ELSEVIER

Composites Science and Technology 61 (2001) 311–319

COMPOSITES SCIENCE AND TECHNOLOGY

www.elsevier.com/locate/compscitech

Digital-element simulation of textile processes

Youqi Wang *, Xuekun Sun

Department of Mechanical and Nuclear Engineering, Kansas State University, Manhattan, KS 66506, USA

Received 26 July 2000; received in revised form 3 October 2000; accepted 17 October 2000

Abstract

This paper establishes the concept of a digital-element. A digital-element model was developed to simulate textile processes and determine the micro-geometry of textile fabrics. It models yarns by a pin-connected digital-rod-element chain. As the element length approaches zero, the chain becomes fully flexible, imitating the physicality of yarns. Contacts between yarns are modeled by contact elements. If the distance between two nodes on different yarns approaches the yarn diameter, contact occurs between them. Yarn micro-structure inside the preform is determined by process mechanics, such as yarn tension and inter-yarn friction and compression. The textile process is modeled as a non-linear solid mechanics problem with boundary displacement (or motion) conditions. First, a simple twisting process is simulated, validating the digital-element model. Then, the yarn geometry of a 3-D, four-step braided preform is analyzed. These numerical results reveal the details of yarn paths within the preform. Such results can only be arduously and expensively obtained when achieved through experimental observation, but cannot be generalized; or are inadequately detailed when achieved through existing analytical methods. This makes it possible, therefore, to conduct a quantitative analysis on the distribution of yarn orientation and fiber volume fraction inside a preform. Yet the value of this new model reaches far beyond that of the braiding process. As a general tool, it is advantageous for other textile processes, such as twisting, weaving and knitting and for the investigation of textile preform deformation during the consolidation process. The new numerical approach described here is identified as digital-element simulation rather than as finite-element simulation because of a special yarn discretization process. With the conventional finite-element approach, the element preserves the physical properties of the discretized body. In contrast, with this model the element itself does not preserve physical properties: physical properties are imitated by the element link. The concept is similar to digital discretization. Therefore, the term 'digital element' is more appropriate. The size of the element must be very small compared to the size normally employed in finite element analysis.

Keywords: Textile composite; Preform mechanics; 3-D braiding process; Finite element; Digital element

1. Introduction

The three-dimensional (3-D) reinforced composite recently arrived in the family of advanced aviation materials. Various textile processes, such as weaving, braiding, stitching and knitting, have been employed to create 3-D composite textile preforms. There are two benefits. Firstly, these processes can yield a near-net-shape product. Secondly and more importantly, fiber structure and mechanical properties can be tailored to meet specific design requirements.

Mechanical properties of textile composites are determined by textile preform micro-structure, such as fiber orientation, fiber-volume fraction, yarn-volume fraction and yarn curvature. Therefore, paramount for the design of 3-D textile composites is the determination of the preform micro-structure.

Two general approaches have been employed to investigate the micro-structure of textile composites. They are:

1. Experimental observation: By cutting a consolidated textile composite specimen along various cross-sections, yarn structure can be observed. SEM and X-ray techniques have been used in the past.
2. Analytical approach: By following the kinematics of the textile process, yarn topology inside the preform can be investigated.

However, the micro-structure of the textile composite is determined not only by kinematics. Yarn trace depends on the mechanics involved in the manufacturing

* Corresponding author. Tel.: +1-785-532-7181.
E-mail address: wang@mne.ksu.edu (Y. Wang).

0266-3538/01/$ - see front matter
PII: S0266-3538(00)00223-2

processes, such as yarn tension and inter-yarn friction and compression. The mechanics in these processes are so complex that it is difficult to find an analytical mathematical solution to describe them. Existing analytical methods [1–8] can only investigate topology. Further, they fail to provide detailed information about the yarn curvature inside the preform.

Experimental observation is expensive and only provides information for the individual preform. Given the complexity of the process and the number of manufacturing parameters, it is incapable of providing guidelines for efficient preform design or of providing the detailed yarn traces needed for composite microstress analysis.

Although the textile process is mechanical, yarn flexibility makes it very difficult to analyze the yarn trace inside the preform by means of conventional solid mechanics methods. For this reason, a digital-element concept is developed in this paper. A digital model is established to simulate various textile processes. It links manufacturing processes to the preform micro-geometry. In this model, yarn is firstly discretized into pin-connected digital elements. Then, the textile process is considered as a non-linear solid mechanics problem with displacement (or motion) boundary conditions. The preform geometry is calculated using digital-element analysis. Details of the digital model will be described later in this paper.

A software package was developed. Initially, a simple twisting case is simulated in order to verify the numerical model and the software package. Then, the numerical model is employed to simulate a 3-D four-step braiding process. The yarn geometry of the braided preform is analyzed. One can visualize the internal yarn paths clearly.

2. Digital-element model

2.1. Concept of digital element and discretization of yarn

In this model, a yarn is considered as a flexible 1-D component with a circular cross-section. It is digitally represented by a set of short cylindrical bars which are connected by frictionless pins, as shown in Fig. 1. These short cylindrical bars are defined as 'two-node digital rod-elements' in this paper. As the length of these digital elements approaches zero, the pin-connected digital-element chain becomes fully flexible, imitating the physical properties of the yarn.

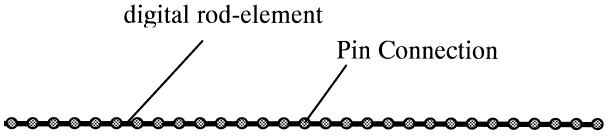

Fig. 1. Discretization of the yarn.

The element is named as 'digital element' rather than 'finite element' because of its special nature.

In conventional finite-element analysis, the element preserves physical properties of the discretized body. Discretization allows us to describe a displacement field (or stress, strain and other mathematical fields) by many localized polynomials. In order to achieve an accurate result, one can choose to use either a smaller element size or a higher order polynomial. The discretization process employed in a finite-element model (FEM) is a mathematical discretization.

In digital-element simulation, the element does not necessarily preserve the physical properties of the discretized body. For example, the elements used to represent a yarn in this model do not preserve the flexible nature of the yarn. Instead, physical properties are imitated by the link (frictionless pin) between these elements. The discretization process employed here is a physical discretization. Generally speaking, the size of the digital elements must be very small, which represents the resolution of the digital analysis. It usually is much smaller than the size of finite elements. Otherwise, physicality (in this case, yarn flexibility) cannot be preserved.

Once the yarn is descritized, the procedure used in conventional element analysis can be used to simulate the textile process.

Stiffness of the digital element can be written as:

$$[K] = \frac{EA}{\Delta L}\begin{bmatrix} 1 & 0 & 0 & -1 & 0 & 0 \\ 0 & 0 & 0 & 0 & 0 & 0 \\ 0 & 0 & 0 & 0 & 0 & 0 \\ -1 & 0 & 0 & 1 & 0 & 0 \\ 0 & 0 & 0 & 0 & 0 & 0 \\ 0 & 0 & 0 & 0 & 0 & 0 \end{bmatrix} \tag{1}$$

where E is the modulus of the yarn, ΔL is the length of the element and A is the area of the cross-section.

In reality, the elongation of the yarn is too small to affect the micro-geometry of the preform. Therefore, yarn stretch can be neglected. If the yarn stretch is not included in the simulation, the term $EA/\Delta L$ can be replaced by a penalty factor G with a large positive value. The stiffness matrixes of all the digital elements can be replaced by the same matrix as following:

$$[K] = \begin{bmatrix} G & 0 & 0 & -G & 0 & 0 \\ 0 & 0 & 0 & 0 & 0 & 0 \\ 0 & 0 & 0 & 0 & 0 & 0 \\ -G & 0 & 0 & G & 0 & 0 \\ 0 & 0 & 0 & 0 & 0 & 0 \\ 0 & 0 & 0 & 0 & 0 & 0 \end{bmatrix} \tag{2}$$

The equilibrium equation in the element coordinate system can be written as follows:

$$[K]\ \{U\} + \frac{1}{2} A\sigma_0\{e\} = \{F\} \tag{3}$$

where σ_0 is the initial tension and

$$\begin{aligned} \{U\} &= \left[U_{xi}\ U_{yi}\ U_{zi}\ U_{xj}\ U_{yj}\ U_{zj}\right]^{\mathrm{T}} \\ \{F\} &= \left[\ F_{xi}\ F_{yi}\ F_{zi}\ F_{xj}\ F_{yj}\ F_{zj}\right]^{\mathrm{T}} \\ \{e\} &= [\ -1\ 0\ 0\ 1\ 0\ 0]^{\mathrm{T}} \end{aligned} \tag{4}$$

2.2. Contact between yarns

Yarns contact each other during the textile forming or the preform deformation processes. As the length of the rod element approaches zero, the contact between two yarns can be represented by the contact of two nodes.

Node m and node l are from two different yarns (Fig. 2). Assume the distance between these two nodes is d_{ml}. Let the diameter of both yarns be D. If $d_{ml} \leqslant D$, contact would occur between these two yarns. A contact element is therefore placed between node m and node l. x-, y- and z-axes are the local coordinates of the contact element. The x-axis is in the direction of the contact line and the y- and z-axes are perpendicular to the contact line. As the element length approaches zero, the x-axis would be perpendicular to both yarns. The contact element can support compression in the x- direction and friction in the y- and z-directions. Each node has three degrees of freedom: displacement in x-, y- and z-directions. An incremental method is used to simulate the contact process.

If contact occurs between two yarns, one of two kinds of physical conditions would exist: sticking or sliding.

Two yarns will stick if $\mu\left|\vec{F}_{xm}\right| > \left|\vec{F}_{ym} + \vec{F}_{zm}\right|$, where μ is the friction coefficient and $\vec{F}_{xm}, \vec{F}_{ym}$ and $\vec{F}_{zm}$ are nodal forces. The relationship between increments of nodal forces and displacements in each sub-step can be written as follows:

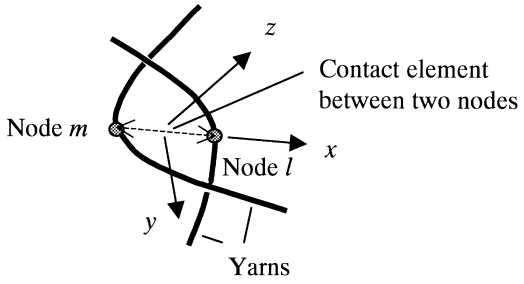

Fig. 2. 3-D contact element.

$$\begin{bmatrix} -k_n & 0 & 0 & +k_n & 0 & 0 \\ 0 & -k_{sy} & 0 & 0 & +k_{sy} & 0 \\ 0 & 0 & -k_{sz} & 0 & 0 & +k_{sz} \\ +k_n & 0 & 0 & -k_n & 0 & 0 \\ 0 & +k_{sy} & 0 & 0 & -k_{sy} & 0 \\ 0 & 0 & +k_{sz} & 0 & 0 & -k_{sz} \end{bmatrix} \begin{Bmatrix} \Delta U_{xm} \\ \Delta U_{ym} \\ \Delta U_{zm} \\ \Delta U_{xl} \\ \Delta U_{yl} \\ \Delta U_{zl} \end{Bmatrix} = \begin{Bmatrix} \Delta F_{xm} \\ \Delta F_{ym} \\ \Delta F_{zm} \\ \Delta F_{xl} \\ \Delta F_{yl} \\ \Delta F_{zl} \end{Bmatrix} \tag{5}$$

where k_n, k_{sy} and k_{sz} are the compression stiffness and the stick stiffness of yarns, respectively. In an elastic contact, they are determined by the yarn's properties. In a rigid contact, displacements of node m and node l are constrained to be the same. Thus, the penalty method can be employed again. A sufficiently large stiffness must be selected in order to prevent the deformation of the yarn's cross-section, yet an unreasonably large value also must be avoided, for that would reduce numerical accuracy.

Sliding occurs between two yarns if $\mu\left|\vec{F}_{xm}\right| \leqslant \left|\vec{F}_{ym} + \vec{F}_{zm}\right|$. Friction between the two yarns is:

$$\left|\vec{F}_{sm}\right| = \left|\vec{F}_{ym} + \vec{F}_{zm}\right| = \mu\left|\vec{F}_{xm}\right| \tag{6}$$

and the nodal forces in the y- and z-directions would be:

$$\begin{aligned} F_{ym} &= \left|\vec{F}_{sm}\right|\cos\alpha_{ysm} \\ F_{zm} &= \left|\vec{F}_{sm}\right|\cos\alpha_{zsm} \end{aligned} \tag{7}$$

where α_{ysm} and α_{zsm} are angles between the sliding direction and the y- and z-directions, respectively. They can be determined by displacements that occurred in the previous sub-step:

$$\begin{aligned} &\cos\alpha_{ysm} = \\ &\left(\Delta U_{ym} - \Delta U_{yl}\right)/\sqrt{\left(\Delta U_{ym} - \Delta U_{yl}\right)^2 + \left(\Delta U_{zm} - \Delta U_{zl}\right)^2} \\ &\cos\alpha_{zsm} = \\ &\left(\Delta U_{zm} - \Delta U_{zl}\right)/\sqrt{\left(\Delta U_{ym} - \Delta U_{yl}\right)^2 + \left(\Delta U_{zm} - \Delta U_{zl}\right)^2} \end{aligned} \tag{8}$$

The relationship between increments of nodal forces and displacements in the x-direction can be written as:

$$\begin{bmatrix} -k_n & k_n \\ k_n & -k_n \end{bmatrix} \begin{Bmatrix} \Delta U_{xm} \\ \Delta U_{xl} \end{Bmatrix} = \begin{Bmatrix} \Delta F_{xm} \\ \Delta F_{xl} \end{Bmatrix} \tag{9}$$

2.3. Singularity treatment

The global stiffness matrix will become singular if any two neighboring digital-rod elements in the system are aligned along the same straight line, as shown in Fig. 3. In order to avoid singularity, two approaches can be adopted.

- Approach 1: stiffness perturbation method

The simplest method to solve the singularity problem is to add small perturbations $\pm\Delta$ to the element stiffness matrix. The element stiffness thus can be written as:

$$[K] = \begin{bmatrix} G & 0 & 0 & -G & 0 & 0 \\ 0 & \Delta & 0 & 0 & -\Delta & 0 \\ 0 & 0 & \Delta & 0 & 0 & -\Delta \\ -G & 0 & 0 & G & 0 & 0 \\ 0 & -\Delta & 0 & 0 & \Delta & 0 \\ 0 & 0 & -\Delta & 0 & 0 & \Delta \end{bmatrix} \tag{10}$$

The absolute value of Δ must be much smaller than G. Yet, an unreasonably small value of Δ must also be avoided, otherwise numerical divergences would be created.

- Approach 2: element merging or displacement perturbation method

When two neighboring elements are aligned along the same straight line, two possible physical conditions could happen (Fig. 4):

a. The middle node does not contact the other yarn, so no external force is applied to the node. Thus, no nodal force is applied to the middle node as shown in Fig. 4(a). The yarn would not be bent at the middle node. Therefore, two elements can be merged and the middle node can be eliminated.
b. The middle node contacts another yarn. Therefore, a contact nodal force is applied to the middle node. This nodal force can be divided into two components: one is in the axial direction, denoted as F_t; whereas, the other is in the normal direction, denoted as F_n. In order to eliminate singularity, a small displacement perturbation δ along the normal direction is first assumed. This small displacement is subtracted in a later calculation step.

The second approach reduces the size of global stiffness, consequently reducing computing time. This also prevents numerical error caused by perturbation $\pm\Delta$. However, the algorithm for the computer code becomes more complex.

The authors adopted the first approach in the software they developed.

2.4. Yarn stability during the textile process

Yarn tension must be positive. Negative yarn tension would cause structural instability of the textile preform. Further, significant numerical error may occur if yarn tension were very small during the process.

2.5. Effectiveness of the numerical model

A simple twisting process was simulated to validate the aforementioned numerical model (see Fig. 5). Fig. 5(a) is the set-up for the twisting process. Two spring elements are placed at the bottom of the yarns in order to maintain yarn tension. First, the top ends of the two yarns are moved upward a distance of Δh to achieve an initial yarn tension. This provides a pre-twist yarn tension. Then, the bottom ends of both spring elements rotate along a circular tract. Thus, a twisted yarn is produced. Fig. 5(b) is the twisted yarn created by digital-element simulation. One also can visualize the

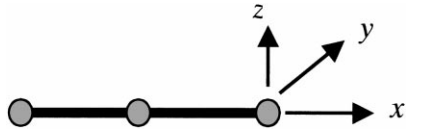

Fig. 3. Digital elements and local coordinate system.

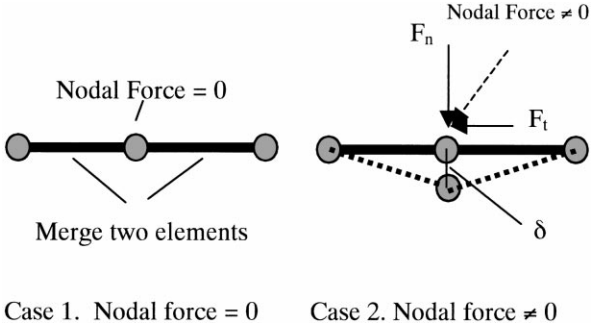

Fig. 4. Special treatment for two aligned neighboring elements.

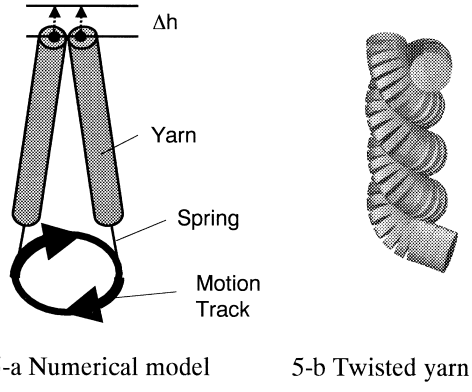

Fig. 5. Digital model and simulation results for the twisting process.

length of the digital elements from Fig. 5(b). The numerical input data used in this example are: yarn diameter $d = 1.96$ mm, $G/\Delta = 10^4$, pre-twist yarn tension = 0.00045 N, spring stiffness = $G/10000$. The length of the digital element = 1/4 d. Friction between yarns are neglected.

3. Micro-structure of 3-D braided composites

The micro-structure of a 1 × 1 four-step 3-D braided composite has been studied by several authors in recent years [1–8]. Li [1,2] observed the internal yarn structure and identified the unit cell of the preform's interior by cutting braided specimens along various cross-sections. Wang and Wang [3–6] investigated the topological structure of the preform. They followed the movement of yarn carriers during the braiding process and traced the yarn path inside the preform. They characterized the general topology of the preform. They concluded that the preform's interior is composed of two basic cells, called cell 'A' and cell 'B'. Both cells 'A' and 'B' contain two yarn segments as shown in Fig. 6(a). The arrangement of cells 'A' and 'B' is shown in Fig. 6(b). It was also found that yarns within interior cells form two families of flat plates: family a and family b [refer to Fig. 6(c)]. Two plates intersect inside the preform as shown in Fig. 6(d). One is formed by cell 'A' and the other by cell 'B'. Yarn arrangement of each plate is similar to a laminated plate. Yarn orientation is characterized by braiding angle γ as shown in the figure. Later, Chen et al. [7,8] observed the yarn trace both inside and on the surface of a preform by using SEM. A similar conclusion about internal yarn structures was reached.

The newly developed digital-element method enabled simulation of the 3-D braiding process and calculation of yarns' spatial paths. In addition to the interior yarn topology, the new method enable us to derive the details of yarn curvature and orientation inside of the preform. This is significant because this affects mechanical properties, such as stiffness, toughness and impact strength.

Fig. 7 shows the initial position of yarn carriers on the machine bed for the numerical simulation. It is set-up to braid a preform with a square cross-section. There are 24 yarns. The carriers move along the horizontal direction and vertical direction alternately. The first step is a horizontal movement. Yarns are divided into four groups. Numbers inside circles identify the group number to which a yarn belongs. Yarns belonging to the same group have similar yarn paths. The numerical model is shown in Fig. 8. It is assumed that friction between yarns is zero and that the cross-section of the yarn remains unchanged inside the preform. The preform

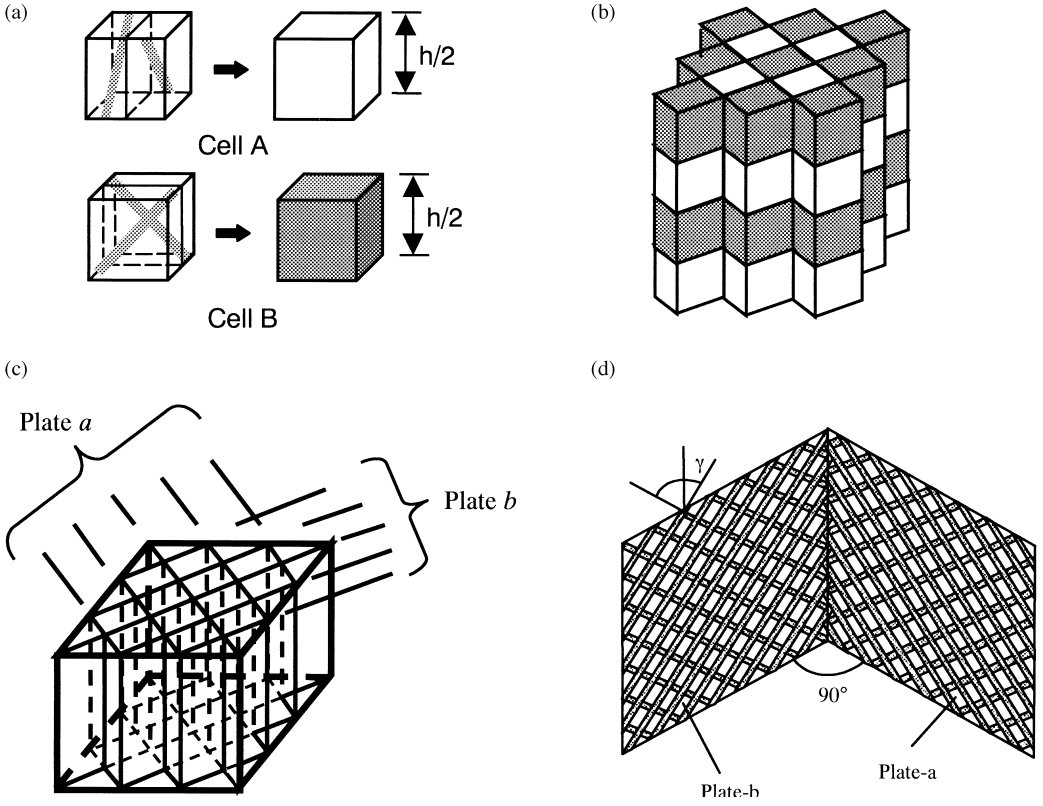

Fig.6. Yarn topology in the preform interior[3]: (a) yarn topology in cells A and B; (b) cell arrangement in the preform interior; (c) two families of plates in the interior; (d) yarn formation and plate intersection.

moves upward at a steady speed as carriers move on the machine bed. Spring elements are placed at the bottom ends of yarns. The yarn diameter is 1.96 mm. $G/\Delta = 10^4$.

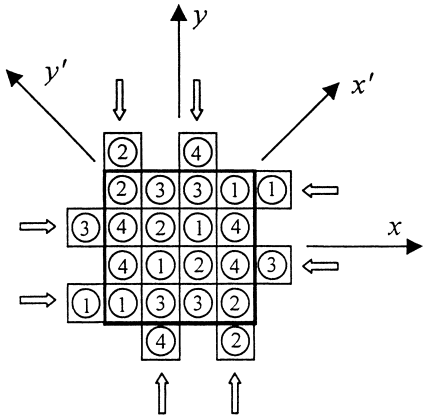

Fig. 7. Braiding set-up.

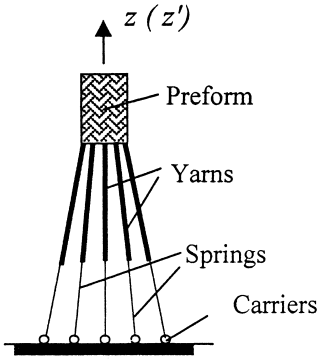

Fig. 8. Numerical model.

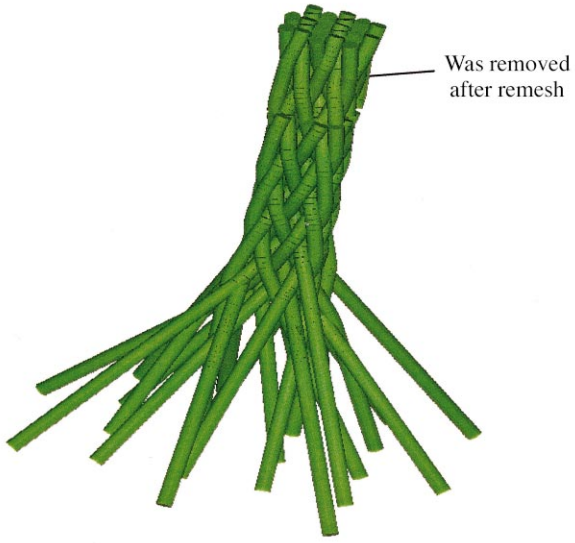

Fig. 9. 3-D preform braided by digital-element simulation model.

The stiffness of the spring element $= G/10^4$. Friction between yarns is neglected. A rigid contact is assumed.

Fig. 9 shows the preform produced by the digital model. Many cycles are needed before yarn paths approach steady state. It was found that the preform's forming process, which occurs at the bottom of the preform, does not affect the micro-geometry of the top portion of the preform. Therefore, the top portion was removed during the braiding process and more yarn elements were periodically added from the bottom. A re-mesh technique was adopted. This procedure was repeated until yarn patterns reached steady state.

In order to observe the interior structure, the preform was cut along the cross-section parallel to the $x'z'$ plane (refer to Figs. 7 and 8). It is shown in Fig. 10. The yarns appear straight inside the preform, bending only at the surface. This was consistent with previous experimental observational results. However, Fig. 11 shows an enlarged projection of yarn paths on the x–y plane. This view clearly shows that yarns curve in a periodic pattern

Fig. 10. $x'oz'$ Cross-section.

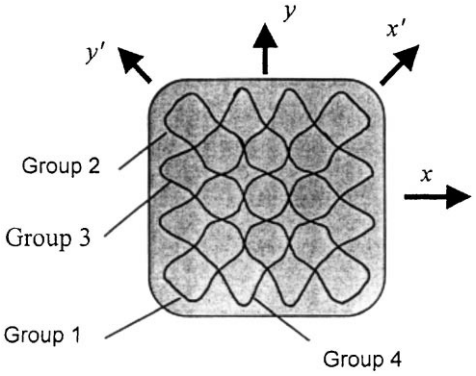

Fig. 11. Projection of yarn traces.

inside the preform. This phenomenon has never been found in pervious research.

We isolated yarns from each group in order to investigate yarn geometry. For example, Figs. 12 and 13 show the isometric view of spatial paths of yarns of groups 1 and group 4, respectively. Yarn paths of groups 2 and 3 are similar to groups 1 and 4, respectively. Projections of a yarn trace from group 1 onto both the $x'z'$ and the $y'z'$ planes are shown in Fig. 14. Likewise, projections of a yarn trace from group 4 onto the same planes are shown in Fig. 15. The pitch length is 13.5 mm. In the $x'z'$ plane, the projection of the yarn remains straight and has a constant angle with the z-axis. The magnitude of this angle is the same as what is defined as the braiding angle according to previous

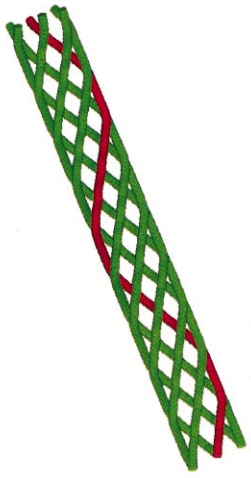

Fig. 12. Spatial traces of yarns of group 1.

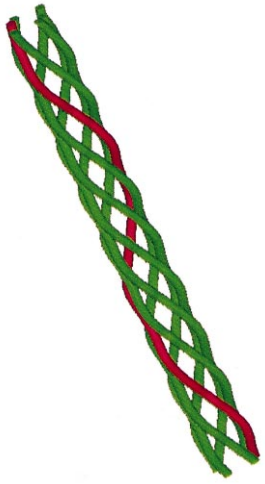

Fig. 13. Spatial traces of yarns of group 4.

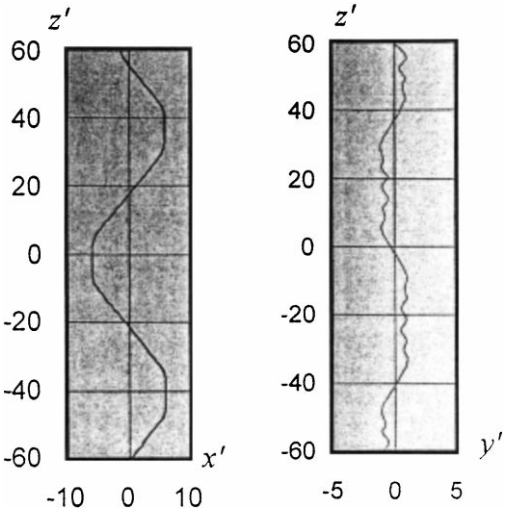

Fig. 14. Yarn path of group 1.

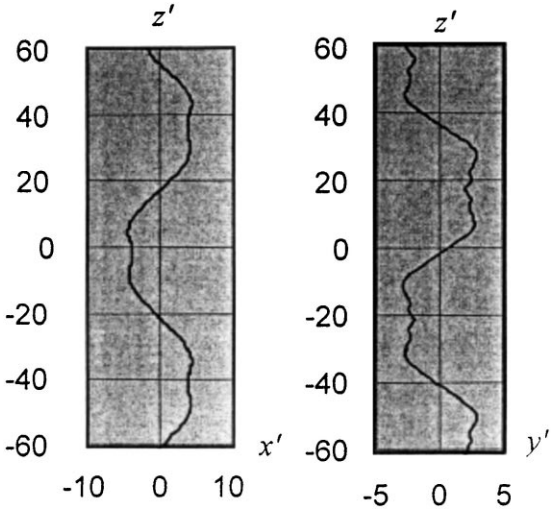

Fig. 15. Yarn path of group 4.

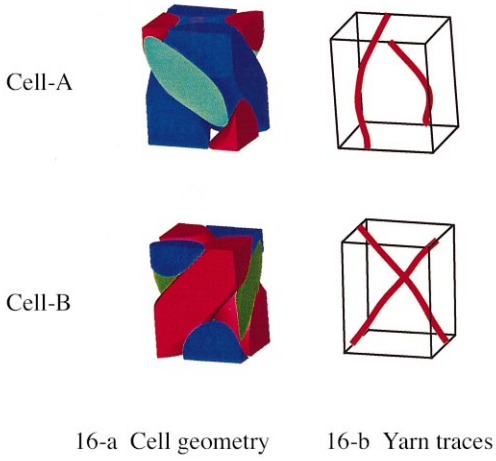

Fig. 16. Microstructure of interior cells: (a) cell geometry; (b) yarn traces.

research. It can be derived from the surface pattern of the preform. However, it is not the actual braiding angle. This is evident when we notice that the yarn projection onto the $y'z'$ plane is curved. Yarn orientation does not remain constant inside the preform. The braiding angle varies with different locations. The curvatures of the yarn depend upon the yarn tension during the braiding process.

In addition, as stated earlier, the interior area of a 3-D preform can be considered as a composition of cells 'A' and 'B'. The isometric view of cells 'A' and 'B' are shown in Fig. 16(a). Each cell contains two curved yarn segments as shown in Fig. 16(b). Readers can compare this with results from the previous research, which is shown in Fig. 6(a).

Fig. 17 shows the microgeometry of the surface and corner cells. The surface cell contains three main yarn segments and the corner cell contains two yarn segments as shown in Fig. 18.

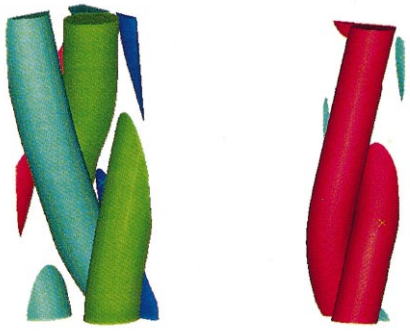

17-a Surface cell 17-b Corner cell

Fig. 17. Micro-structure of boundary cells: (a) surface cell; (b) corner cell.

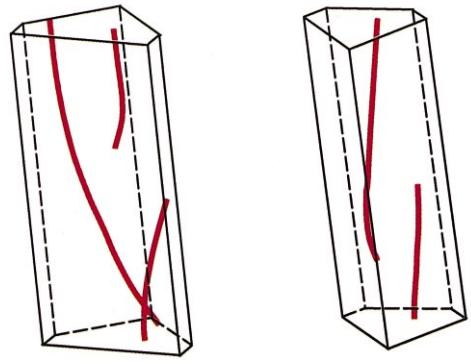

18-a Surface cell 18-b Corner cell

Fig. 18. Yarn traces in boundary cells: (a) surface cell; (b) corner cell.

4. Concluding remarks

This paper establishes the concept of a digital element. A digital model was developed to simulate textile processes.

The digital element employed does not preserve the physical properties of yarns. The element stiffness matrix used in this paper is simple. In fact, all digital-rod elements can share the same stiffness matrix, which is shown in Eq. (5). The yarn's physicality, i.e. flexibility, is imitated by the frictionless pin-node. Therefore, the length of the yarn must be very small. Otherwise, the physical properties of the yarn can not be imitated. The length of the digital element used in numerical examples is 1/4 of the yarn diameter.

The yarn paths of a 3-D braided preform were studied in detail. The curvilinear state of yarns in the interior area is characterized. This significantly expands our knowledge about the micro-geometry of 3-D braided preforms. The digital tool developed in this research enables us to quantitatively investigate the yarn trace inside the preform. The curvilinear state of yarns significantly affects the mechanical properties of composites, such as stiffness, toughness and impact strength.

Yarn spatial paths and fiber-volume fractions within preforms are affected by yarn friction coefficients, yarn tension, yarn transverse compression stiffness, the distance between machine bed and preform and other manufacturing parameters. However, relationships between detailed yarn geometry and manufacturing parameters lie outside the purview of this paper. That will be published elsewhere.

The digital-element model can be applied not only to simulate the textile process, but also to investigate the preform deformation that occurs during the consolidation process. It is an important advancement in textile preform mechanics.

Acknowledgements

The authors would like to acknowledge AFOSR financial support. The authors thank Professor Prakash Krishnaswami at Kansas State University for his insights into the computer code post-process. Dr. Pagano's helpful discussions are also acknowledged.

References

[1] Li W. On the structural mechanics of 3-D braided preforms for composites. PhD thesis, North Carolina State University, 1990.
[2] Li W, Hammad M, Shiekh AE. Structural analysis of 3-D

braided preforms for composites. Journal of Textile Institute 1990;81:491–514.
[3] Wang YQ, Wang ASD. On the topological yarn structure in 3-D rectangular and tubular braided performs. Journal of Composites Science and Technology 1994;51:575–86.
[4] Wang YQ, Wang ASD. Microstructure-property relationships in 3-D braided composites. Journal of Composites Science and Technology 1995;53:213–22.
[5] Wang YQ, Wang ASD. Geometric mapping of yarn structures in 3-D braided composites due to shape change. Journal of Composites Science and Technology 1995;53:359–70.
[6] Wang YQ, Wang ASD. Spatial distribution of yarns and thermomechanical properties in 3-D braided tubular composites. Journal of Applied Composite Materials 1997;4:121–32.
[7] Chen L, Tao XM, Choy CL. On the microstructure of three-dimensional braided performs. Journal of Composites Science and Technology 1999;59:391–404.
[8] Chen L, Tao XM, Choy CL. Mechanical analysis of 3-D braided composites by the finite multiphase element method. Journal of Composites Science and Technology 1999;59:2383–91.